## Ultrasensitive nonlinear vibrational spectroscopy of complex molecular systems

Selig, O.

**Publication date**
2017
**Document Version**
Other version
**License**
Other

# Chapter 8

# Organic Cation Rotation and Immobilisation in Pure and Mixed Methylammonium Lead-Halide Perovskites

**Three-dimensional lead-halide perovskites have attracted a lot of attention due to their ability to combine solution processing with outstanding optoelectronic properties. Despite their soft ionic nature these materials demonstrate a surprisingly low level of electronic disorder resulting in sharp band edges and narrow distributions of the electronic energies. Understanding how structural and dynamic disorder impacts the optoelectronic properties of these perovskites is important for many applications. Here we combine ultrafast two-dimensional vibrational spectroscopy and molecular dynamics simulations to study the dynamics of the organic methylammonium (MA) cation orientation in a range of pure and mixed tri-halide perovskite materials. For pure $MAPbX_3$ (X=I, Br, Cl) perovskite films, we observe that the cation dynamics accelerate with decreasing size of the halide atom. This acceleration is surprising given the expected strengthening of the hydrogen bonds between the MA and the smaller halide anions, but can be explained from the increase in the polarizability with the size of halide. Much slower dynamics, up to partial immobilisation of the organic cation, are observed in the mixed $MAPb(Cl_xBr_{1-x})_3$ and $MAPb(Br_xI_{1-x})_3$ alloys, which we associate with symmetry breaking within the perovskite unit cell. The observed dynamics are essential for understanding the effects of structural and dynamical disorder in perovskite-based optoelectronic systems.**

## 8.1 INTRODUCTION

Hybrid organic-inorganic perovskite materials have recently attracted significant attention because devices made from these materials show outstanding optoelectronic properties while the fabrication procedures are themselves very simple, for example, spin coating followed by low-temperature annealing.[196,241,242] Films of methylammonium lead iodide ($MAPbI_3$) are among the most investigated materials in the family of the 3D perovskites because they demonstrate a particularly high potential for use in thin-film solar cells with certified power conversion efficiencies exceeding 21%.[196,243] At the same time, the ease with which the bandgap of this compound can be tuned by merely changing the ionic composition opens up a whole new dimension for possible optoelectronic applications.[197,244] The bandgap can be tuned across the entire visible spectrum by varying the nature of the halide ions from $I^-$ to $Br^-$ and $Cl^-$, which makes this material particularly promising for tandem solar cell, light emitting diode (LEDs) and laser applications.[197,198,244–247] A precise and gradual control of the band structure is achieved in the mixed halide $MAPb(Cl_xBr_{1-x})_3$ and $MAPb(Br_xI_{1-x})_3$ systems. It has been recently shown that specific combinations of ions lead to the formation of alloys with well-defined intermediate-size bandgaps, surprisingly sharp band edges, and narrow distributions of emissive states.[244,248]

The structural properties of such 'soft' hybrid perovskite materials are expected to lie at the core of their optoelectronic performance. Interionic interaction opens many degrees of freedom and allows molecular motions on multiple time and length scales.[249] There are various ways in which the structural dynamics of hybrid perovskites could affect their optoelectronic properties, and to date a number of such potentially important effects have been predicted and/or observed,[250–257] including bandgap and exciton binding energy modulation,[258] ferroelectric alignment,[259,260] polaronic localisation of excited states,[251,261] charge transport[262] and assistance in water percolation.[263]

Relatively limited information is available about the molecular-scale dynamics in these systems despite their clear importance. The motions are expected to occur on multiple timescales, and these include both ultrafast cation rotations and vibrational motions of the inorganic lattice. It is worth pointing out that these structural dynamics may be heterogeneous and may vary throughout the material depending on the microscopic composition and local structure of the perovskite. All this calls for advanced spectroscopic methods and theoretical approaches able to identify and interpret the complex variety of molecular-level processes. Substantial progress towards understanding the dynamics of $MAPbI_3$ materials was achieved using a range of techniques[264] including simulations,[265,266] quasi-elastic neutron scattering,[225,267,268] NMR[217] as well as electronic[269] and vibrational[270–272] spectroscopy. At the same time, less is known about the structural dynamics of the $Br^-$ and $Cl^-$ systems.[273] Even fewer studies have focused on the mixed perovskites and the question as to how the structure of these materials changes as a function of their composition.[274–276]

In the previous chapter, we developed a method to directly track the orientational dynamics of the MA cations within the lead-halide lattice. We applied this method

to $MAPbI_3$ films and observed two characteristic time constants of motion. Using ab-initio molecular dynamics simulations, we identified the observed dynamics as (i) fast (∼300 fs) 'wobbling-in-a-cone' motions of the MA ions around the crystal axes and (ii) relatively slow (∼3 ps) jump-like reorientations of the organic ions with respect to the lead-iodide lattice. Within our ∼10 ps experimental window we did not witness any long-term orientation memory nor pronounced immobilisation of the MA cations. We found no evidence for the suggestion in the literature that the rearrangement of the MA would be responsible for the hysteretic behaviour observed in perovskite photovoltaic devices.[221,224]

Here we extend our previous approach to the chloride- and bromide- perovskites, as well as to mixed-halide systems. We observe that for pure $MAPbI_3$, $MAPbBr_3$ and $MAPbCl_3$ films the cation dynamics accelerate with decreasing size of the halide atom and consequent shrinking unit cell of the crystal. We observe a stronger slowing, down to a partial immobilisation of the cation, in the mixed $MAPb(Cl_xBr_{1-x})_3$ and $MAPb(Br_xI_{1-x})_3$ alloys. We associate these slower dynamics with a symmetry breaking in the unit cell. We speculate that cation immobilisation can affect the local dielectric environment and contribute to the increased static but decreased dynamic disorder in mixed-halide perovskite materials.

## 8.2 RESULTS AND DISCUSSION

### 8.2.1 LINEAR INFRARED SPECTROSCOPY

All samples used in this study were prepared by A. Sadhanala, C. Müller, R. Lovrincic and Z. Chen. Figure 8.1 shows the IR absorption spectra of the pure and mixed perovskite films under study. Here we focus on the region 1350–1700 $cm^{-1}$ where the strongest mode (∼1475 $cm^{-1}$) corresponds to the $NH_3^+$ bending vibrations.[230] The bimodal structure of the absorption bands originates from the splitting of three degenerate vibrations into one symmetric (∼1475 $cm^{-1}$) and two antisymmetric (∼1580 $cm^{-1}$) normal modes. The low-frequency peak corresponds to the symmetric mode whose transition dipole moment is aligned with the C–N axis of the MA molecule. Following the work in the previous chapter, we use the transient anisotropy of this vibration to monitor the rotational dynamics of the organic cation. We see that the frequency of the symmetric $NH_3^+$ bending vibration of the MA cation decreases with increasing size of the halide anion. There are two effects that probably contribute to this redshift. The first effect is the decreasing strength of the $NH\cdots X^-$-hydrogen bond with increasing size of the $X^-$ anion, because bending vibrations typically show a positive correlation between hydrogen-bond strength and frequency.[277] The second effect that contributes to the observed redshift is a particular local-field effect described in ref.[230] Specifically, the MA vibrations redshift due to the fact that they are embedded inside and interact with a polarizable medium—the lead-halide lattice, whose polarizability increases with increasing anion size.[230] The vibrational absorption spectrum of $MAPb(Cl_xI_{1-x})_3$ can be represented as a linear superposition of the absorption spectra of $MAPbI_3$ and $MAPbCl_3$. This is in agreement with previous reports,

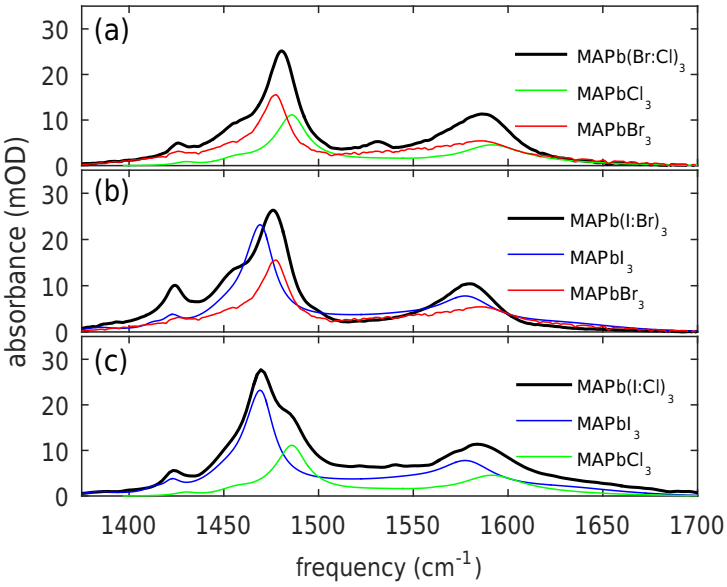


FIGURE 8.1. Linear infrared spectra of the studied materials. Every panel shows the spectrum of one hybrid sample and the corresponding pure halide spectra (a) $MAPb(Cl_{0.35}I_{0.65})_3$ , (b) $MAPb(Br_{0.6}I_{0.4})_3$ and (c) $MAPb(Cl_{0.6}Br_{0.4})_3$.

showing that $MAPb(Cl_xI_{1-x})_3$ does not form a homogeneous mixture but phase segregates into pure iodide and chloride phases.[278,279] In contrast, the vibrational spectra of $MAPb(Br_xI_{1-x})_3$ and $MAPb(Cl_xBr_{1-x})_3$ contain a single narrow peak for each mode, positioned between the vibrational frequencies observed for the pure halide systems. This corroborates the previous observation that these halides are well mixed at the level of the perovskite unit cell; the MA ions experience a homogenous and relatively narrow distribution of local environments[244,248]

### 8.2.2 2DIR SPECTROSCOPY OF PURE-HALIDE PEROVSKITES

To study the orientational dynamics of the organic cations, we performed 2DIR anisotropy experiments on the symmetric $NH_3^+$ bending vibration of the MA ions. Detailed information about the experimental configuration can be found in Chapter 3. Briefly, 2DIR spectroscopy can be viewed as a version of infrared pump-probe spectroscopy, in which the transient signals are recorded as a function of both the probe and the pump frequency. This allows one to study phenomena such as mode coupling and vibrational energy transfer[77,238] In addition, the fact that the signal is spread along two frequency dimensions allows for a better separation of multiple, overlapping, resonances compared to pump-probe spectroscopy. Polarization-resolved detection of the probe pulse allows for disentanglement of the 2DIR signal into an isotropic and anisotropic contribution. The former gives direct access to the relaxation dynamics, and the latter allows one to track the reorientation of the

transition dipoles (and thereby the orientational motions of chemical groups). For example, the transition dipole of the symmetric $NH_3^+$ bending vibration is aligned with the C–N axis of the MA cation, so that the transient anisotropy decay of this transition follows the orientation of the cation.

Figure 8.2 shows the isotropic 2DIR spectra of the studied materials. Two dominant features can be seen in every spectrum: a negative (orange) peak originating from the depletion of the vibrational ground state and stimulated emission from the first excited state; and a positive (blue) peak at a lower frequency due to excited state absorption (ESA). Interestingly, in all samples except $MAPb(Cl_xI_{1-x})_3$, the 2D lineshapes are symmetric and show no elongation along the diagonal, which points to weak inhomogeneous broadening of this vibrational mode. This lack of diagonal elongation (i.e. inhomogeneous broadening) suggests that the MA ions experience a narrow distribution of local environments in both $MAPb(Br_xI_{1-x})_3$ and $MAPb(Cl_xBr_{1-x})_3$. In contrast, $MAPb(Cl_xI_{1-x})_3$ shows a pronounced elliptical line shape which can be interpreted as a superposition of the 2DIR spectra of the chloride and iodide perovskites. We observe no sign of cross peaks between the chloride and iodide components, which confirms the presence of strong phase segregation[279] as well as a lack of interaction (or interconversion) between the MA cations in the different phases. In the previous chapter, we showed that the region around the ground-state bleach might be affected by a thermal response which makes it difficult to extract the molecular reorientation from this signal. Consequently, we focus on the anisotropy dynamics of the ESA region, which is not affected by the thermal signal. Figure 8.3(a) shows the transient anisotropy dynamics averaged over the central region of the excited state absorption (ESA) peaks for the pure-halide perovskites. In general, the dynamics involve two components similar to those which we have previously attributed to a confined wobbling (~300 fs) of the MA molecules and to jump-like reorientations between the halide unit cell facets. In order to extract the time constants associated with these motions we have fitted the previously used wobbling-in-a-cone relaxation model to the anisotropy decays. The resulting jump rates, cone semi-angles, and wobbling time constants are summarized in Table 1. Perhaps surprisingly, the general trend observed is that as we move to smaller halide atoms and smaller unit cell sizes (from $I^-$ to $Br^-$ and then to $Cl^-$) the reorientation of the MA ions accelerates. This acceleration is primarily due to the increased probability for the occurrence of large-angle jumps; the fast process associated with the wobbling motion seems unaffected and can be well described by the same time constant for all five samples. This can be understood in terms of the large-angle jumps being driven by the tilting modes of the inorganic perovskite cage, whereas the wobbling-motion is a characteristic of the molecule rattling within the inorganic cage.[280,281] The variation of the time constant for the large scale jumps qualitatively agrees with the shift in frequency for the coupled cage-organic modes.[282]

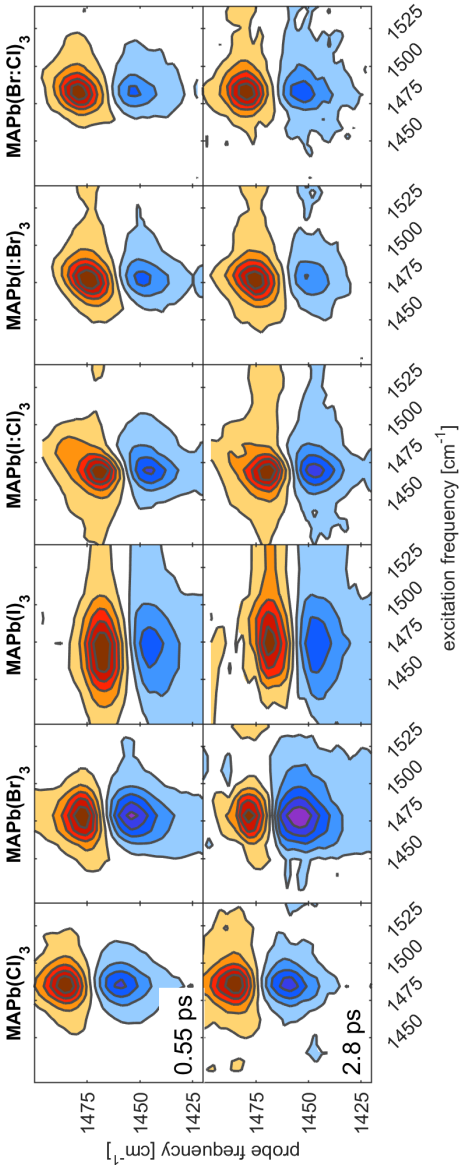


FIGURE 8.2. Isotropic 2D spectra for the studied materials at two different evolution times. The contour lines are placed at steps of 20% of the maximum amplitude. Red colors indicate negative absorption changes while blue colors indicate positive absorption changes.

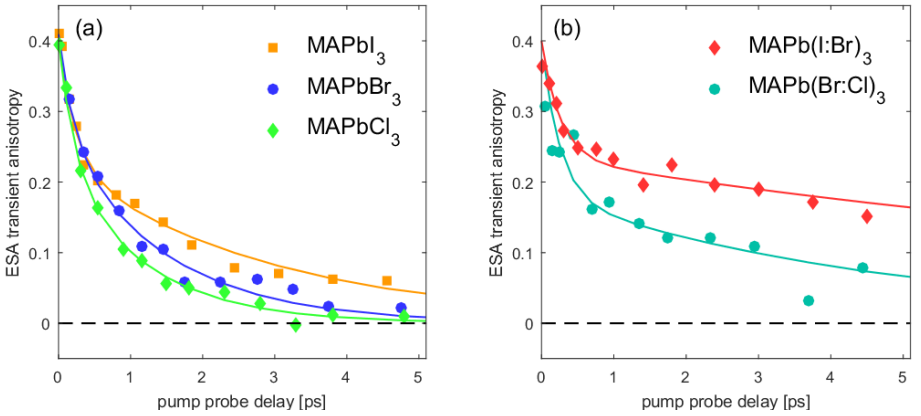


FIGURE 8.3. Transient anisotropy dynamics of the $MA^+$ ion as measured in the centre of the ESA for the $NH_3{}^+$ bending mode. The solid symbols show the experimentally determined anisotropy for the pure-halide perovskites in a) and for the mixed-halide perovskites in b). The lines show the fit with the wobbling-in-a-cone relaxation model.

| Perovskite | Θ (°) | $\tau_{wob}(ps)$ | $\tau_{jump}$ (ps) |
|---|---|---|---|
| $MAPbI_3$ | 34 | 0.3 | 3.0 |
| $MAPbBr_3$ | 29 | 0.3 | 1.5 |
| $MAPbCl_3$ | 34 | 0.3 | 1.2 |
| $MAPb(I:Br)_3$ | 34 | 0.3 | 14.3 |
| $MAPb(Br:Cl)_3$ | 40 | 0.3 | 5.0 |

TABLE I. Results of fitting the transient anisotropy data of all measured perovskite samples withe the jump/wobbling-in-a-cone relaxation model: $R(t) = 2/5e^{-t/\tau_{jump}}(S^2 + (1-S^2)e^{-t/\tau_{wob}})$ with $S = \cos(\Theta)(1+\cos(\Theta))/2$, , where $\Theta$ is the semi-cone angle, $\tau_{wob}$ and $\tau_{jump}$ are the wobbling and angle jump times scales, respectively.

### 8.2.3 MOLECULAR DYNAMICS SIMULATIONS OF PURE-HALIDE PEROVSKITES

In order to support our experimental findings T. C. Jansen and J. M. Frost have performed classical polarizable MD simulations with a $6 \times 6 \times 6$ unit cubic super cell. They have used these simulations to compute the second-order correlation function of the MA orientations. This correlation function is proportional to the experimentally determined transient anisotropy and is expressed as

$$R(t) = \frac{2}{5}\langle(\hat{\mu}(t)\cdot\hat{\mu}(0))\rangle \tag{8.1}$$

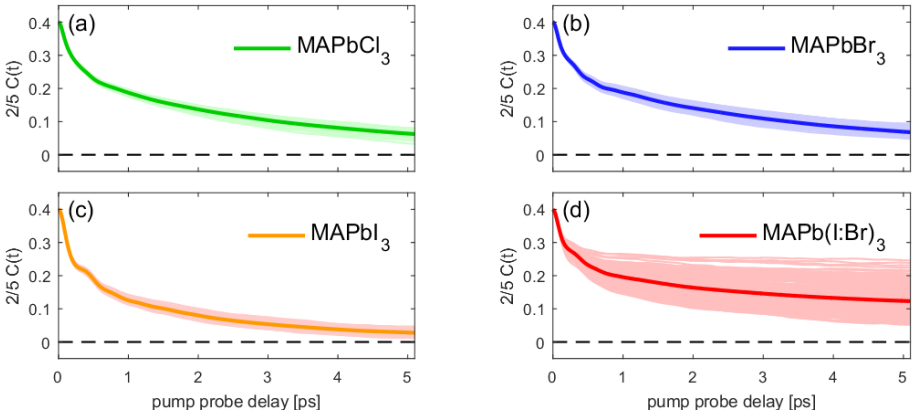


FIGURE 8.4. Rotational correlation functions of the MA ions as calculated based on classical molecular dynamics simulations for the pure-halide perovskites $MAPbCl_3$ (a), $MAPbBr_3$ (b) $MAPbI_3$ (c) and for the mixed-halide perovskite $MAPb(I:Br)_3$ (d). The faint lines represent the individual correlation functions for the different MA ions in the simulation while the thick lines represent the average over the complete calculated ensemble.

where $P_2(x)$ is the 2nd Legendre polynomial, $\hat{\mu}(t)$ is a unit vector pointing along the C–N-axis of the MA ion, and $\langle \ldots \rangle$ denotes an ensemble average. Clearly the anisotropy curves extracted from the MD trajectories show the same two-component dynamics as the experimental anisotropies (Figure 8.4(a)-(c)), however, the change of time scale for the slow component with respect to the change of the size of the halide ions is not reproduced.

At first sight it may seem surprising that the reorientation of the MA ions speeds up along the series $MAPbI_3 \rightarrow MAPbBr_3 \rightarrow MAPbCl_3$ because, as was already mentioned above, the NH···$X^-$ hydrogen bond should strengthen when one moves in this direction. However, it should be realized that it is not the absolute strength of the hydrogen-bond, which determines the reorientation rate, but rather the activation barrier for moving between two equivalent hydrogen bonded orientations of the MA cation. This activation barrier is due to the fact that in the transition state the hydrogen bond is slightly elongated compared to the stable positions. Apparently the energy penalty for lengthening the hydrogen-bond in the transition state decreases in the direction $MAPbI_3 \rightarrow MAPbBr_3 \rightarrow MAPbCl_3$. This is probably due to the fact that the unit cell size decreases for this series, which in turn causes the potential confining the MA ions to become more spherically symmetric. A similar situation is encountered in the reorientation of water where molecules engaging in so-called bifurcated hydrogen bonds represent a low-energy transition state which speeds up reorientation.[283–285] The activation energy is apparently not well reproduced by the molecular dynamics simulations. This may not be surprising as the force field was not optimized for reproducing this. With a difference in rate in the order of a factor 2 this corresponds to a difference in the 2.5 kJ/mol range for the activation energy.

In the picture sketched above, we have described the reorientation of the MA ion

as an activated process, and we have attributed the change in reorientation rate to a change in activation barrier. However, the rate of an activated process is not only determined by the height of activation barrier but also by the dynamic changes in this barrier. Recent X-ray scattering experiments and DFT calculations suggested a moderate to strong coupling between the deformation or the inorganic lattice and the rotational motion of the organic cation.[225,281] Therefore, one could imagine that the reorientation of the MA ion is facilitated by the low-frequency vibrations of the lead-halide lattice. In this scenario, the modulation of the barrier (attempt frequency) for rotational motions is directly given by the frequency of these lattice vibrations. Recent infrared and Raman experiments have shown that the frequency of these lattice modes typically increases along the series $MAPbI_3 \rightarrow MAPbBr_3 \rightarrow MAPbCl_3$,[262,274,282] and this trend would be in line with the observed increased in the MA reorientation rate. Summarizing, according to this interpretation the speeding up of the MA reorientation with decreasing size of the halide anion is attributed to two effects that work in the same direction: an increasing influence of lead-halide lattice vibrations and a decreasing activation barrier. Next we turn to the mixed-halide perovskites.

### 8.2.4 2DIR SPECTROSCOPY OF MIXED-HALIDE PEROVSKITES

Figure 8.3(b) presents the transient anisotropy recorded at the centre of the ESA peaks for the $MAPb(Br_xI_{1-x})_3$ and $MAPb(Cl_xBr_{1-x})_3$ alloys. We do not discuss the anisotropy of the $MAPb(Cl_xI_{1-x})_3$ system as the linear and 2DIR spectra of this compound system show a trivial superposition of the chloride and iodide components (see Appendix Sec. 8.4, and Fig 8.2). The short-time dynamics in $MAPb(Br_xI_{1-x})_3$ and $MAPb(Cl_xBr_{1-x})_3$ are similar to those in the other pure- and mixed-halide systems, which indicates that the wobbling motions are well activated in all these materials. However, at longer time delays significantly slower anisotropy decays are observed for the mixed-halide perovskites, compared to the pure-halide perovskites. This slowing down indicates that the molecular jumps between different unit cell facets are strongly suppressed in the mixed-halide materials and that each individual MA cation remains predominantly oriented in a particular direction. This immobilisation can be understood by considering the activation energy for the rotational motion (similarly to the pure-halide systems). For the mixed-halide systems the halide lattice site is occupied by a statistical mixture of two halide ions. As a consequence the different MA orientations will no longer be characterized by identical hydrogen-bond strengths (as was the case for the pure-halide systems). Instead the statistical, usually asymmetric, distribution of the halide ions will lead to the presence of specific MA orientations which have an energetic minimum in their rotational potential. For these MA orientations the activation energy for a 90-degree jump will obviously be much larger compared to the case of the pure-halide perovskites, for which reorientation between stable positions is not associated with a change in hydrogen-bonding energy. This means that the random substitution of halogen sites within the inorganic cage effectively generates an asymmetric pocket which pins down the orientation of the MA ions.

### 8.2.5 MOLECULAR DYNAMICS SIMULATIONS OF MIXED-HALIDE PEROVSKITES

The mixed perovskites were modelled by T. C. Jansen using classical polarizable molecular dynamics simulations. This allowed using 6x6x6 super cells with 216 organic cations to obtain sufficient sampling of the different halogen environments. The halogen atoms were inserted in a statistical manner resulting in a heterogeneous distribution of unit cells with $x = 0.6$. Organic cations with anywhere from 3 to 11 $Br^-$ ions in the first coordination sphere were found. Figure 8.4(d) presents the rotational correlation function for a set of individual MA cations (in the mixed $MAPb(Br_xI_{1-x})_3$ perovskite) as well as the overall ensemble average. As clearly seen from the individual pink transients the distribution of correlation functions is very broad for the mixed-halide systems, in contrast to the narrow distribution for individual cations in the pure-halide perovskites (Figure 8.4 (a)-(c)). As a general trend the jump time was found to be slower for cations surrounded by an equal number of $Br^-$ and $I^-$ ions than for cations in a more homogeneous environment. Considering the number of possible ways to construct these unit cells and the fact that every cation can form three hydrogen bonds, a complete analysis of the factors determining the slowdown was not possible. However, we can generally state that altering the symmetry of the unit cell should provide anisotropy and the preferred direction for the cation orientation. Changing the orientation in such way that the number of hydrogen bonds to a particular type of halogen is preserved should be more favourable as compared to when the type of halogen is changing. Interestingly, the observed immobilisation of the organic cation in mixed-halide perovskites correlates with a number of trends previously observed in material properties. For example, previous studies indicated that both the emissive bandwidth and the Urbach energy are persistently smaller in pure-halide systems compared to their respective mixtures.[244,248] Similar trends are observed in the structural measurements like XRD and in the charge transporting properties.[276] All these observations point to an increased level of disorder in mixed-halide systems compared to pure-halide systems. Our new results indicate that, at least as far as the organic cation is concerned, the static and dynamic disorders change differently upon mixing different halide ions in the material. The static disorder is clearly increased in mixed halide systems as observed in the elongation of 2D peaks in Figure 2.[286] At the same time, the dynamic motions are clearly suppressed by breaking the symmetry of the unit cell. With suppressed dynamics, the static dielectric constant will decrease (the molecules can no longer respond) potentially explaining the higher exciton binding energy reported for mixed $MAPb(Br_xI_{1-x})_3$ perovskites.[287] While we do not have direct evidence to associate the change in electronic properties with the variations in the cation dynamics, we believe that the observed correlation manifests a clear link between electronic and structural dynamics in perovskite materials.

## 8.3 CONCLUSION

We presented a 2D IR and MD simulation study of the orientational dynamics of the organic cation in a range of pure- and mixed-halide perovskite materials. In the pure halide materials $MAPbCl_3$, $MAPbBr_3$ and $MAPbI_3$ we observe that the reorientation of the organic cation slows down with increasing halide size. We ascribe this trend to a decreasing probability of the MA to perform large-angle jumps. In the mixed $MAPb(Cl_xBr_{1-x})_3$ and $MAPb(Br_xI_{1-x})_3$ alloys we observed a higher degree of static disorder and much slower structural dynamics down to partial immobilisation of the organic cations. We associate these effects with the symmetry breaking within the halide unit cell. The observed effects of the halide composition on the structural and dynamical properties of perovskite materials may be partly responsible for the previously observed variations in their optical and electronic properties.

# 8.4 APPENDIX

## LINEAR COMBINATION OF FTIR SPECTRA

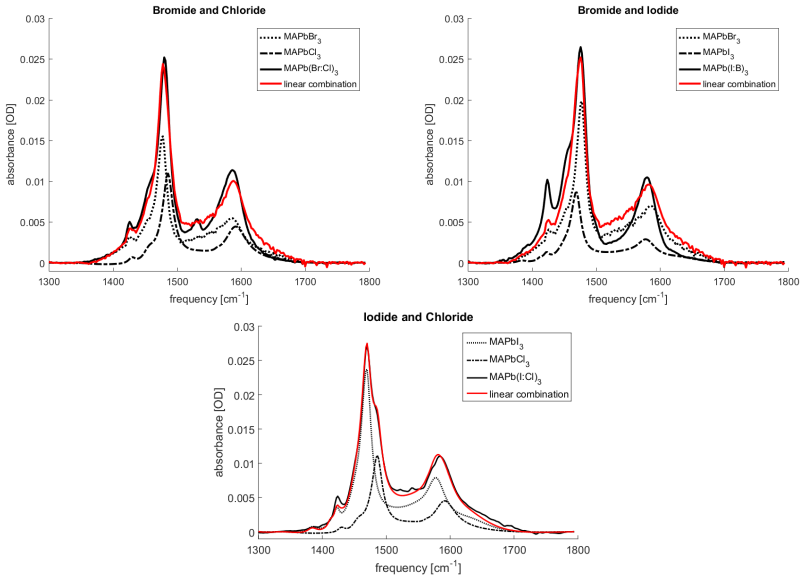


FIGURE 8.5. Comparison between the FTIR spectra of the mixed-halide perovskites and the best matching linear combination of the corresponding pure-halide perovskites spectra.

## REPRESENTATIVE 2DIR DATA

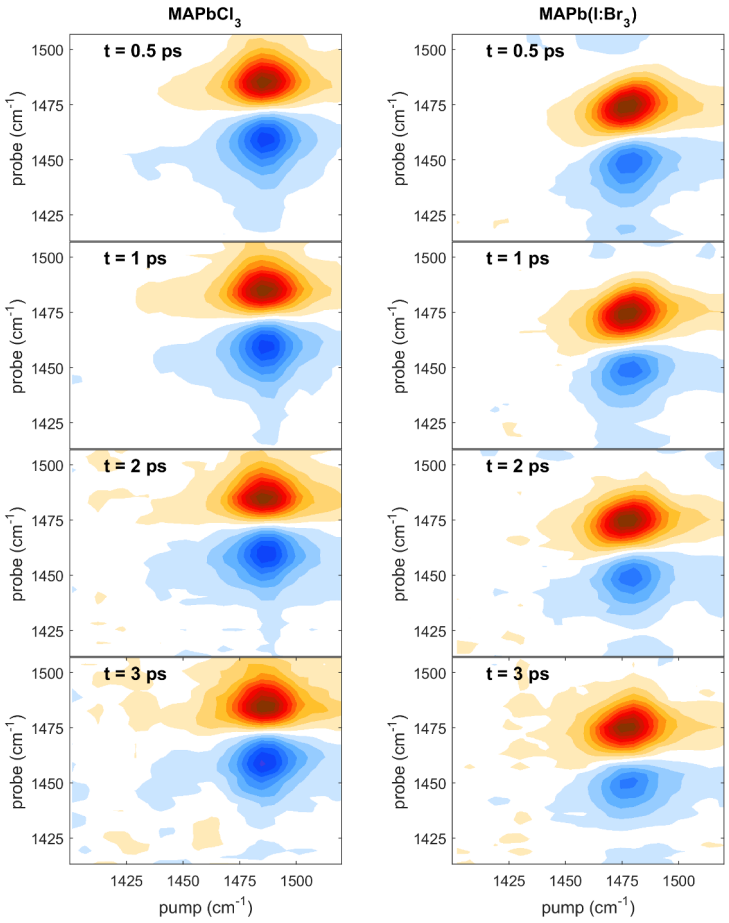


FIGURE 8.6. Typical 2DIR maps at different evolution times (isotropic component). The contour lines are positioned at steps of 10% of the maximum amplitude.

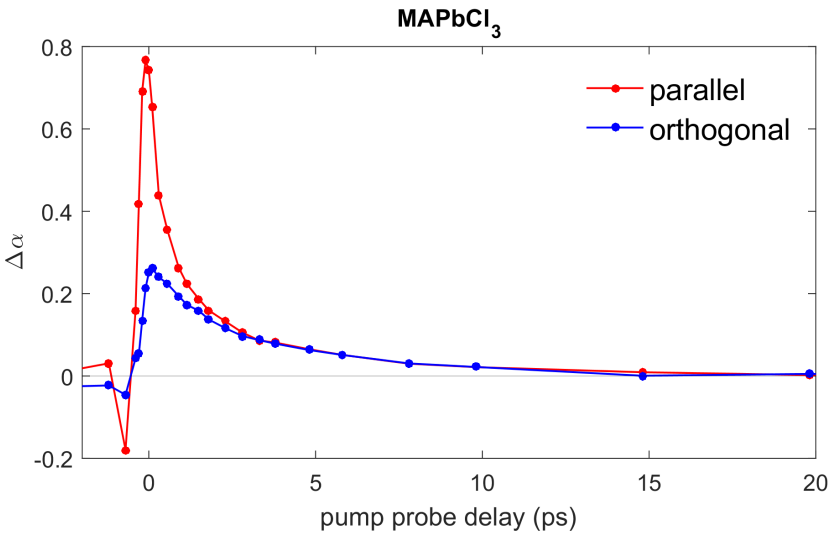


FIGURE 8.7. Typical absorption change in the ESA peak measured with parallel and orthogonal polarization of the probe pulse relative to the pump pulse. Lines are guides to the eye.